GROOVE FORMATION ON PHOBOS FROM ORBITAL EJECTA OF STICKNEY CRATER. X. Xi[1,2], M. Ding[1,2] and M.-H. Zhu[1,2], [1]State Key Laboratory of Lunar and Planetary Sciences, Macau University of Science and Technology, Macau, China (miding@must.edu.mo), [2]CNSA Macau Center for Space Exploration and Science, Macau, China.

Introduction: The surface of Phobos is almost entirely covered by linear groove features. The grooves can been classified according to their distributions and morphologic characteristics (e.g., 1-2). Several scenarios have been proposed to explain the formation of these grooves, including the strong drag force when Phobos was captured by Mars [3], impact fracturing due to the Stickney impact event [4], and secondary crater chains caused by Mars ejecta [2,5]. However, no single mechanism can explain the formation of all these classes of observed grooves [e.g., 6]. Instead, multiple scenarios may be required to explain their spatial distribution and morphologic characteristics.

One of the leading hypotheses for the groove formation considers the effect of Stickney impact ejecta. Wilson & Head [7] and Ramsley & Head [8, 9] suggested one subset of the grooves are caused by suborbital Stickney crater ejecta with relatively low launch velocity (3-8 m/s) that can slide, roll, and bounce on the surface of Phobos. In contrast, Nayak & Asphaug [10] and Nayak [11] predicted crater chains due to orbital ejecta with relatively high launch velocity re-impacting Phobos.

Here we suggest that these high-velocity orbital ejecta, if associated with sufficient horizontal velocity component when re-impacting Phobos, may also slide on the surface of Phobos and create groove-like linear features. We simulate the formation of the Stickney crater and its impact ejecta distribution. The launch velocities of these impact ejecta are then used for calculating their trajectories based on path integration. For the orbital ejecta re-impacting Phobos, we apply the sliding boulder model [7] to calculate the ejecta paths. The modeled paths are then compared with observed groove patterns to test their association with the orbital ejecta from the Stickney crater.

Simulation of Stickney Crater Formation: In order to investigate impact ejecta from the Stickney crater, we use the multi-material, multi-rheology iSALE-2D shock physics code [12,13] to model the impact cratering process and track ejecta distribution. We then track ejecta trajectories during the impact cratering process, and record the launch positions and velocities when the ejecta leave from Phobos' surface [14-17]. Since the impact hydrodynamic model is two-dimensional, we symmetrically rotate the recorded launch positions and velocities of the impact ejecta particles with respect to the crater center to obtain a corresponding three-dimensional distribution for subsequent calculations.

Ejecta Trajectory Calculation: After selecting the ejecta particles with velocities comparable to or larger than the Phobos' escape velocity, we calculate their trajectories using numerical path integration by considering gravitational perturbations of both Mars and Phobos in a Phobos-Mars coordinate system following [18,19]. The ellipsoid shape of Phobos and Coriolis force are taken into account. The fates of the considered ejecta particles are expected to fall into four categories: re-impacting Phobos, re-impacting Mars, orbiting Mars, or leaving the Martian system. This study is focused on the ejecta re-impacting Phobos. We test two orbital altitudes of Phobos to consider the uncertainty in the formation time of the Stickney crater: the current orbital altitude for a younger formation age of ~ 2.6 Ga, and an altitude of 1.2 times the current altitude for an older formation age of ~ 4.2 Ga [20].

Groove Formation Quantification: When the re-impact ejecta particles strike on a rubble-pile structure with thick regolith like Phobos, the kinetic energy after the re-impact is expected to be reduced by a considerate amount. This energy reduction can be quantified by a speed restitution coefficient $\varepsilon = v_r/v_i$, where v_r and v_i represent the retained speed after and before re-impact, respectively. We test ε in a range of 0.1-0.5 [21].

We then apply the sliding boulder model [7] to predict the length of grooves potentially produced by re-impact ejecta, wherein the length of the ejecta path is positively correlated to the ejecta radius r and retained sliding (horizontal) speed v_r, and negatively correlated to the depth-width ratio of the ejecta path a. The variables r and a are tested in a range of 25-150 m and 0.1-0.2. For the re-impact ejecta particle to slide on the surface for a considerable length and form the observed linear grooves, we only consider re-impact ejecta particles with re-impact angles less than 20°.

Results and Comparison with Observations: Our trajectory calculations show that only ~ 1% of the total ejecta particles re-impacts Phobos, and potentially produces groove-like features. Their space trajectories are highly different. For the current orbital altitude of Phobos, about 45% of these particles follow a simple ballistic sub-orbital trajectory before landing on Phobos' surface within an hour (e.g., Particles A, B in Fig. 1). The rest ~ 55% of the re-impact particles, associated with higher initial launch speeds, temporarily

become satellites orbiting Phobos before re-impacting Phobos at 1-5 hours after launch (e.g., Particles C-E in Fig. 1).

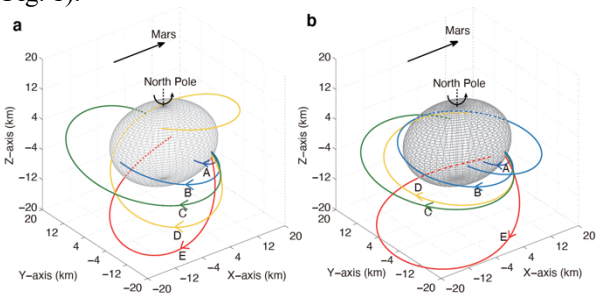

Figure 1. Five typical trajectories for test particles A-E from the Stickney crater (a) assuming the current Phobos' orbital altitude and (b) assuming a Phobos' orbital altitude 1.2 times the current value. The launch speeds are 5.9 and 10.7 m s^{-1} for A and B, and 11.9 m s^{-1} for C-E.

The space trajectories of the orbital ejecta determine their landing positions and velocities back on Phobos. Our calculated landing positions for re-impacting ejecta with a re-impact angles less than 20° are shown by dots in Fig. 2. These ejecta particles are only located in restricted areas at longitudes of ~ 30°, 120°, 210°, and 330°. Based on their re-impact velocity, our predicted ejecta paths using the sliding boulder model [7] are shown by colored curves in Fig. 2. Here the calculated ejecta paths assume a best-fit ejecta radius (r) of 150 m, depth-width ratio of the path (a) of 0.1, and speed restitution coefficient (ε) of 0.3, in order to match the observed groove length of 10-20 km base on the Phobos Viking Global Mosaic Image (e.g., 22).

Our predicted sliding direction of the re-impact ejecta particles from ~ 30° and 210° longitudes is from east to west, while those particles from ~ 120° and 330° longitudes follow an opposite sliding direction. Based on the observed change in the width and depth of groove features, it can be inferred that the corresponding ejecta moves from east to west in the region to the east of the zone of avoidance, while the ejecta move in an opposite direction in the region to the east of the Stickney crater [see ref. 6]. Therefore, our predicted groove direction matches the inferred direction in the former region, but cannot explain the groove direction in the latter region. The grooves in the latter region are likely formed by the Stickney ejecta with relatively low velocities that are smaller than the escaping velocity of Phobos [7].

When the orbital altitude of Phobos increases to 1.2 times the current value, the space trajectories of orbital ejecta particles become longer (Fig. 1b) due to lower gravitational force of Mars. Our predicted ejecta paths on Phobos also become shorter and more restricted in the equatorial region with higher re-impact angles (Fig. 2b). Albeit the above differences, both orbital altitudes can explain the observed groove features in the region to the east of the zone of avoidance (Fig. 2).

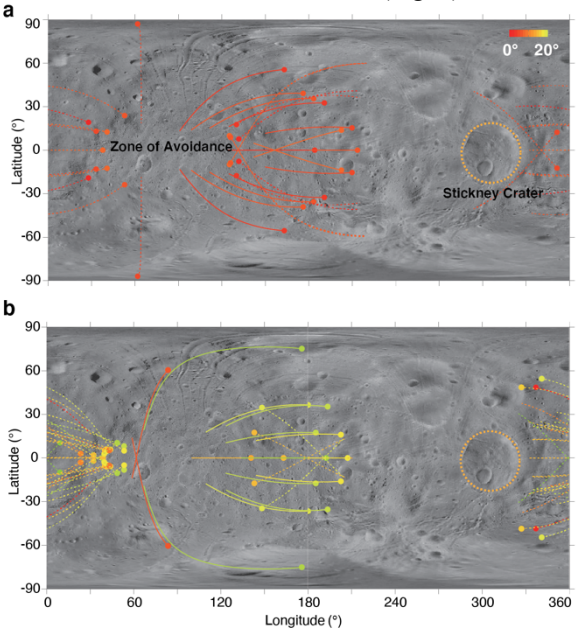

Figure 2. Distribution of our calculated groove-like ejecta paths on Phobos in the current orbital altitude case (a) and 1.2 times current orbital altitude case (b) assuming best-fit parameters. The solid dots are landing positions of re-impact ejecta. The different colors represent different re-impact angles, controlling ejecta path lengths. The background is from Phobos Viking Global Mosaic Image [22].

Acknowledgements: This work was supported by the Science and Technology Development Fund, Macau (0020/2021/A1, 0079/2018/A2) and NSFC 12173106.

References: [1] Thomas P. C. et al. (1979), *J. Geophys. Res.*, *84*, 8,457-8,477. [2] Murray J. B. & Iliffe J. C. (2011), in *Martian Geomorphology*, 21-41. [3] Pollack J. B. & Burns J. A. (1977), *Bull. Am. Astron. Soc.*, *9*, 518-519. [4] Fujiwara A. & Asada N. (1983), *Icarus, 56*, 590-602. [5] Ramsley K. R., & Head J. W. (2013), *Planet. Space Sci.*, *75*, 69-95. [6] Murray J. B. & Heggie D. C. (2014), *Planet. Space Sci.*, *12*, 119-143. [7] Wilson L. & Head J. W. (2015), *Planet. Space Sci.*, *105*, 26-42. [8] Ramsley K. R. & Head J. W. (2017), *Planet. Space Sci.*, 138, 7-24. [9] Ramsley K. R. & Head J. W. (2019), *Planet. Space Sci., 165*, 137-147. [10] Nayak M. & Asphaug E. (2016), *Nat. Comms., 7*, 1-8. [11] Nayak M. (2018), *Icarus*, *300*, 145-149. [12] Collins G. S. et al. (2004), *Meteorit. Planet. Sci.*, *39*, 217–231. [13] Wünnemann K. et al. (2006), *Icarus, 180*, 514-527. [14] Wünnemann K. et al. (2016), *Meteorit. Planet. Sci., 51*, 1,762-1,794. [15] Zhu M. -H. et al. (2015), *J. Geophys. Res.*, *120*, 2,118-2,134. [16] Zhu M. -H. et al. (2017), *Geophys. Res. Lett.*, *44*, 11,292-11,300. [17] Zhu M. -H. et al. (2019), *J. Geophys. Res., 124*, 2,117-2,140. [18] Davis D. R. et al. (1981), *Icarus, 47*, 220-233. [19] Banaszkiewicz M. & Ip W. -H. (1991), *Icarus, 90*, 237-253. [20] Thomas P. C. (1998), *Icarus, 131*, 78-106. [21] Çelik O. et al. (2019), *Space Sci., 178*, 104693. [22] Stooke P. (2012). Stooke Small Bodies Maps V2.0. NASA Planetary Data System.